

**$10^4 - 10^6$  K IONIZED GAS IN THE LARGE MAGELLANIC CLOUD**

You-Hua Chu

Astronomy Department, University of Illinois  
1002 W. Green Street, Urbana, IL 61801, USA**RESUMEN**

La Nube Mayor de Magallanes (NMM) es una de las dos galaxias en las cuales el gas interestelar ionizado, con temperatura de  $10^4 - 10^6$  K, y la población de estrellas masivas embebidas pueden ser estudiados con resolución espacial de sub-parsecs en toda la galaxia. Nuestra habilidad para estudiar este gas en la NMM se ha visto incrementada por el desarrollo de los observatorios espaciales *ROSAT*, *ASCA*, *HST*, e *IUE*. Los estudios existentes de absorción interestelar en el UV en la NMM confirman la existencia de gas a  $10^5$  K en grandes superburbujas y cáscaras supergigantes, pero no permiten verificar la existencia de un halo gaseoso continuo. Observaciones recientes en rayos X, tomadas con el *ROSAT*, muestran gas a  $10^6$  K en grandes estructuras del tipo cáscara así como en regiones no asociadas con estas estructuras. Se discute la relación existente entre las componentes a  $10^4$ ,  $10^5$  y  $10^6$  K a varias escalas de tamaño.

**ABSTRACT**

The Large Magellanic Cloud (LMC) is one of the only two galaxies in which the  $10^4 - 10^6$  K ionized interstellar gas and its underlying massive stellar population can be studied with a sub-parsec resolution over the entire galaxy. Our ability to study the hot ionized gas in the LMC has been enhanced by the availability of the space-based *ROSAT*, *ASCA*, *HST*, and *IUE* observatories. Existing UV interstellar absorption line studies of the LMC confirm the existence of  $10^5$  K gas in large superbubbles and supergiant shells, but cannot conclude on the existence of a continuous hot gaseous halo of the LMC. Recent *ROSAT* X-ray observations of the LMC show  $10^6$  K gas in large shell structures as well as in regions not associated with any interstellar structures. The relationship among the  $10^4$ ,  $10^5$ , and  $10^6$  K components is discussed for interstellar structures at various scale sizes.

**Key words:** MAGELLANIC CLOUDS — ISM: BUBBLES — ISM: SUPERNOVA REMNANTS X-RAYS: INTERSTELLAR — H II REGIONS

**1. INTRODUCTION**

The Magellanic Clouds (MCs) present the best laboratories to study the physical processes in the interstellar medium (ISM). They have several advantages that can not be matched by any other galaxy. They are near enough that their interstellar structures can be studied in great detail; they are also far enough that the entire galaxy can be viewed clearly and studied easily with existing optical and X-ray observing facilities. Their small inclination angles minimize the confusion, and their small foreground and internal obscuration maximize the visibility. Most importantly, massive stars in the MCs can be individually resolved so that interstellar structures can be studied in conjunction with the underlying massive stellar population to achieve a comprehensive understanding of their evolution under one ecosystem.

The Large Magellanic Cloud (LMC) is the more interesting of the two MCs because it contains more interstellar gas and massive stars. It is also the simpler of the two because it is not as tidally stretched. Therefore, we have chosen the LMC as our laboratory to study the interplay between the ISM and massive

stars. We have begun collecting multi-wavelength data and building our knowledge of the ISM and massive stars. Our final goal is to understand the physical structure and evolution of the entire ISM in the LMC and use this knowledge to decipher physical phenomena observed in distant galaxies.

In this paper, I will first divide the hot ionized interstellar gas into  $10^4$  K,  $10^5$  K, and  $10^6$  K components and review the database available and our current understanding (§ 2). I will then divide the interstellar structures according to their scale sizes, describe observations of their hot gas content, and discuss their implications (§ 3). Future work is briefly described in § 4.

## 2. AVAILABLE DATABASE OF HOT IONIZED GAS IN THE LMC

Interstellar structures produced by energetic events, such as stellar winds and supernova remnants (SNRs), usually contain ionized gas at temperatures that span nearly four orders of magnitude,  $10^4$  to  $\sim 10^7$  K. These different temperature components need to be studied at different wavelengths. Usually the  $10^4$  K component is best detected in the optical  $H\alpha$  emission line, the  $10^5$  K component in the UV interstellar N V, C IV, and Si IV absorption lines, and the  $10^6 - 10^7$  K component in the soft X-ray emission.

### 2.1. $10^4$ K Ionized Gas

The  $10^4$  K gas in the LMC has been surveyed extensively using  $H\alpha$  images taken with photographic plates (Henize 1956; Davies, Elliott, & Meaburn 1976, hereafter DEM). A photographic multi-emission-line survey of the LMC, including  $H\alpha + [N II]$ ,  $[O III]$ , and  $[S II]$  lines, was carried out by Lasker (1979) on the Curtis Schmidt telescope, but only low-resolution prints were available in the CTIO Contributions. Photometry of LMC H II regions has been done using PDS scans of  $H\alpha$  and red continuum photographic plates taken with the Curtis Schmidt telescope (Kennicutt & Hodge 1986) or photoelectrically using a Fabry-Perot scanner (Caplan & Deharveng 1985). Recently, a low-resolution  $H\alpha$  CCD image of the LMC was used to study large-scale interstellar structure and star formation (Kennicutt et al. 1995). This  $H\alpha$  image is reproduced in Figure 1.

Two on-going surveys of the  $10^4$  K ionized gas in the LMC will provide an extremely useful database in the future: the imaging Fabry-Perot  $H\alpha$  survey at ESO by Laval et al. (1994) and the multi-emission-line CCD survey using the CTIO Curtis Schmidt telescope by Smith et al. (1995). The F-P survey has a  $9''$  pixel size and a  $38' \times 38'$  field-of-view; it provides both flux and velocity information for the entire LMC, and will be useful for studies of nebular dynamics as well as global kinematics. The multi-emission-line CCD survey consists of images with  $1.1 \times 1.1$  field-of-view in five filters:  $H\alpha$ ,  $[O III]$ ,  $[S II]$ , blue continuum, and red continuum. The resolution will be about  $2''$  pixel $^{-1}$ . This survey, expected to be largely completed by early 1996, will be very useful in identifying faint nebulosities and providing excitation diagnostics.

### 2.2. $10^5$ K Ionized Gas

The  $10^5$  K ionized gas is not as easily studied as the hotter or cooler gas because it emits mostly in the UV where the interstellar extinction is high. Under most interstellar conditions, the  $10^5$  K gas can be diagnosed only in the interstellar N V, C IV, and Si IV absorption lines against background UV sources, such as early-type stars or quasars. Therefore, studies of the distribution of the  $10^5$  K gas are severely limited by the availability of probes against which interstellar N V, C IV, and Si IV absorption lines can be measured.

The *International Ultraviolet Explorer (IUE)* archive contains a large number of high-dispersion spectra of LMC targets. Most of the observations have been optimized for adequate UV fluxes, hence the probes are mostly early-type stars that are in OB associations and embedded in H II regions or superbubbles. These data can be used to confirm that superbubbles and supergiant shells in the LMC do contain  $10^5$  K ionized gas, but cannot be used to probe whether there is a continuous hot halo around the LMC (Chu et al. 1994).

### 2.3. $10^6$ K Ionized Gas

$10^6 - 10^7$  K gas can be studied in soft X-rays. The *Einstein* survey of the LMC detected a large number of small sources associated with X-ray binaries and SNRs, and several large-scale diffuse sources associated with H II complexes, a supergiant shell, and others (Wang et al. 1991). The launch of the *ROSAT* X-ray satellite provides an opportunity to view the LMC in unprecedented resolution and sensitivity. Snowden & Petre (1994) have mosaiced the pointed Position Sensitive Proportional Counter (PSPC) observations, and presented an excellent X-ray image of the LMC. A B/W version of this X-ray image is presented in Figure 2. We may compare

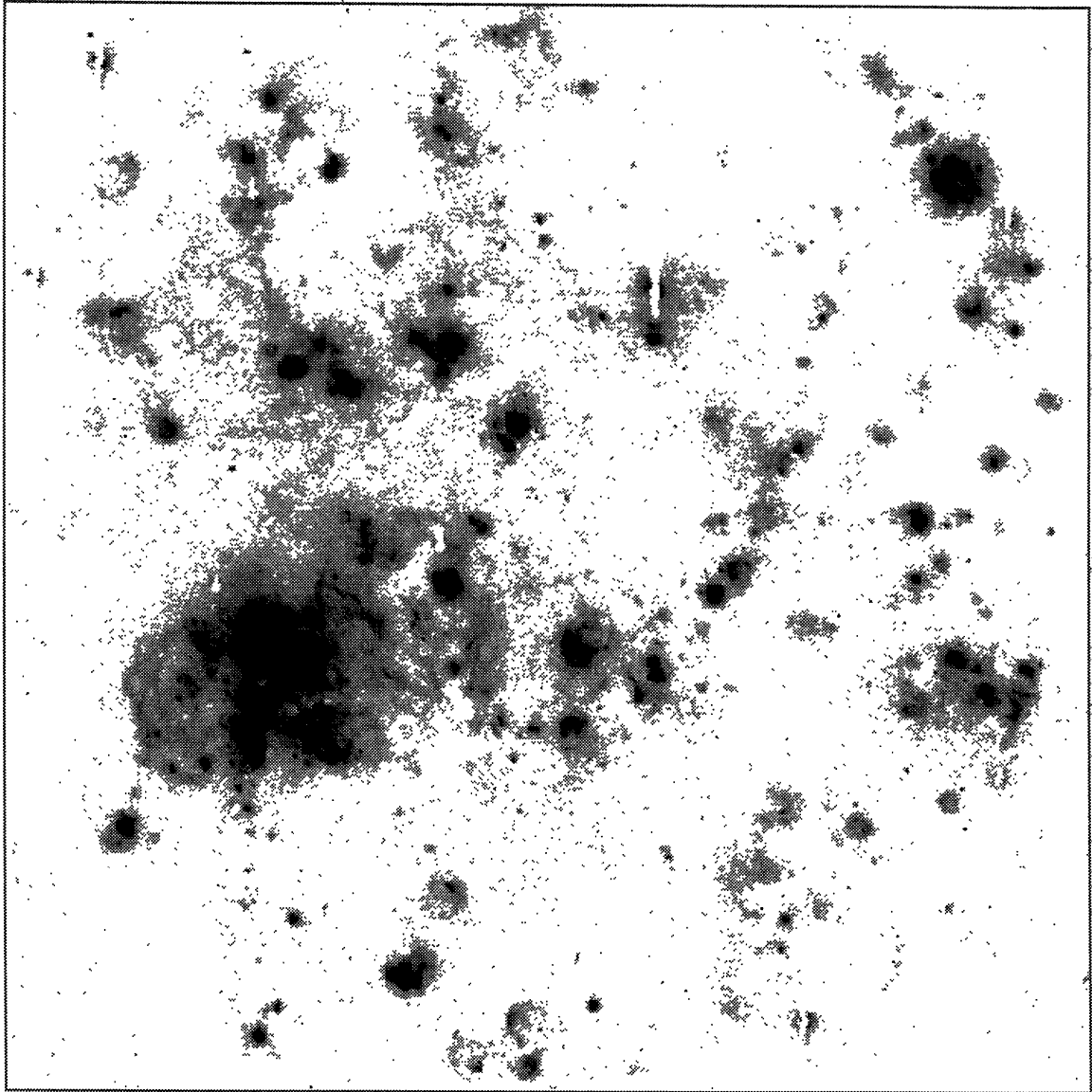


Fig. 1.  $H\alpha$  image of the Large Magellanic Cloud. Reproduced from the image published by Kennicutt et al. (1995). Courtesy of R. C. Kennicutt. The field is roughly the same as the field in Figure 2.

Figures 1 and 2 to see the relationship between the diffuse X-ray emission and the interstellar structures. The bright small sources are X-ray binaries, SNRs, and superbubbles. The large-scale diffuse emission is clearly visible. Some of the diffuse emission is associated with supergiant shells, such as LMC2 and LMC3, while others do not seem to be associated with any visible interstellar structure, such as the emission along the LMC bar. Most of the X-ray emission probably originates from hot gas, some might be from unresolved stellar sources, especially at places where stellar density is high. The on-going *ROSAT* High Resolution Imagery (HRI) survey of the LMC (Chu et al. 1995c) can resolve and detect point sources at a limit of  $\sim 1 \times 10^{34}$  erg  $s^{-1}$ . The survey results will be used to remove contaminating point sources in the PSPC mosaic for a more accurate analysis of the diffuse emission from hot plasmas.



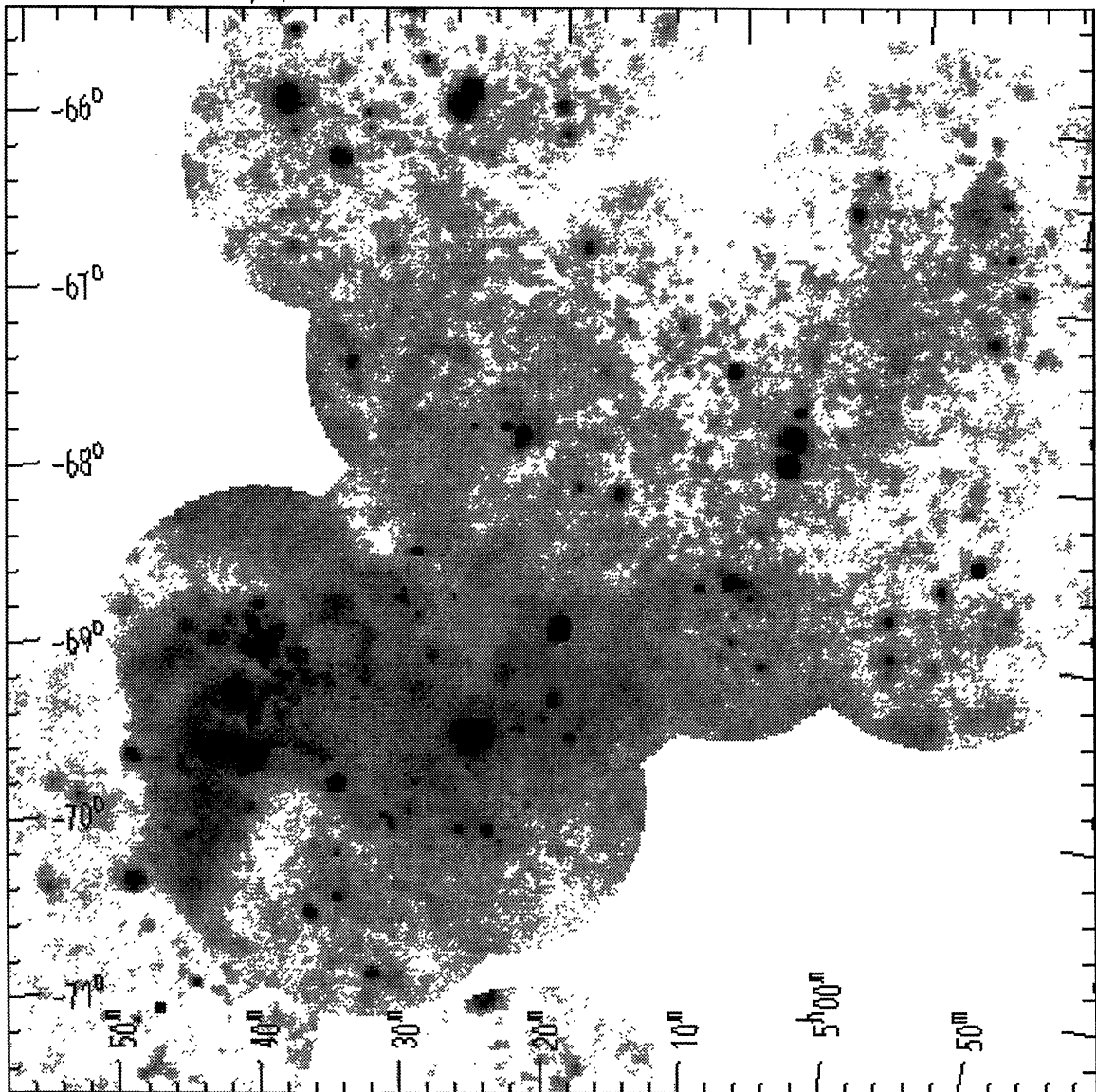


Fig. 2. X-ray mosaic of the Large Magellanic Cloud in the R4-R7 band,  $\sim 0.5 - 2.0$  keV. Reproduced from the image published by Snowden & Petre (1994). Courtesy of S. Snowden.

### 3. HOT IONIZED GAS IN INTERSTELLAR STRUCTURES AT DIFFERENT SCALE SIZES

In principle, both stellar winds and SNRs can produce hot ionized gas; however, in practice, the hot gas produced by SNRs emits more intensely and is much easier to detect than that associated with shocked stellar winds. For example, only one or two wind-blown bubbles have been detected in X-rays, while most SNRs are identified because of their bright X-ray emission. In this section I will discuss the hot gas content of the interstellar structures of different scale sizes in the LMC and the scientific information that can be derived from observations of the hot gas.

### 3.1. Supernova Remnants

The LMC contains a large number of SNRs: 32 have been cataloged by Mathewson et al. (1983, 1984, 1985) using *Einstein* X-ray survey results, and four more have been uncovered by *ROSAT* observations (Chu et al. 1993; Smith et al. 1994; Chu et al. 1995a). These SNRs form an ideal sample to study systematically the physical structure and evolution of SNRs. X-ray observations of SNRs reveal the distribution and amount of hot gas within them. As a Ph.D. project, R. Williams is analyzing the *ROSAT* and *ASCA* X-ray observations of LMC SNRs to determine the physical conditions and thermal energies in their interiors. Most of these SNRs have CCD images and echelle observations to allow the determination of their shell kinetic energy. Therefore, her study will show directly how isolated SNRs inject energy into the ISM and contribute to the 10<sup>6</sup> K hot phase of the ISM.

### 3.2. Superbubbles

Superbubbles are the large shell structures (50 – 200 pc diameter) formed by the combined action of stellar winds and supernovae from a large number of OB stars, such as an OB association. The physical structure of a superbubble is very similar to that of a bubble blown by the stellar wind from a single star (Weaver et al. 1977). Inside, the stellar winds are adiabatically shocked to 10<sup>6</sup> – 10<sup>7</sup> K; outside, the ambient ISM is shocked and radiatively cooled to a 10<sup>4</sup> K shell. At the contact surface between the shocked wind and the shocked ISM, mass evaporation and heat conduction take place, enhancing the density and hence X-ray emission of the shocked-wind layer. If the ISM is clumpy, dense interstellar clumps, having lagged behind the swept-up shell of inter-clump medium and being engulfed in the hot interior, will provide more contact surfaces for heat conduction and mass evaporation to enhance the density and X-ray emission of the superbubble interior.

However, superbubbles are more complicated than single-star bubbles because of the possible existence of interior SNRs. If a SNR interacts with only the hot tenuous interior, the supernova energy will go into the thermal energy of the hot interior and heat further the already hot medium; no observable effects are produced. If a SNR reaches the dense shell walls, pronounced X-ray emission may be produced and other signatures of shocks may become observable (Chu & Mac Low 1990). Alternatively, if the ISM is clumpy, an interior SNR may ablate the embedded clumps and produce observable X-ray emission (Arthur & Henney 1995).

The large number of superbubbles in the LMC provide perfect testing grounds for these different models of superbubble structures. It is important to differentiate these different models, not only because these are fundamental astrophysical problems but also because they predict different physical condition and evolution of superbubbles which ultimately determine the global evolution of the ISM. It is not always straightforward to differentiate these models; however, some progress has been made for the X-ray-dim and X-ray-bright superbubbles.

At least four LMC superbubbles appear to be X-ray-dim, DEM31, DEM105, DEM106, and DEM137. The *ROSAT* PSPC observations are deep enough to yield meaningful upper limits on their X-ray emission. The upper limits are consistent with those expected from Weaver et al.'s models in a homogeneous medium, thus excluding a clumpy medium or additional SNR heating in these four superbubbles (Chu et al. 1995b).

Some LMC superbubbles are so bright in X-ray that they have been detected by the *Einstein* survey (Chu & Mac Low 1990; Wang & Helfand 1991a). Their X-ray luminosities are more than an order of magnitude higher than those expected in Weaver et al.'s models, so off-center SNRs have been proposed to explain the excess X-ray emission. However, based on the X-ray information alone, the clumpy medium explanation — with or without SNRs — cannot be ruled out completely.

It may be possible to differentiate these different models if the 10<sup>5</sup> K gas component at the contact surfaces is observed, using C IV or N V absorption lines against the UV spectra of stars at the center of a superbubble. These different models predict different velocities of the C IV and N V absorption lines relative to the H $\alpha$  emission line velocity of the approaching side of the superbubble. For example, the model with a clumpy medium without any SNRs would produce C IV and N V absorption at velocities similar to the approaching side the shell velocity, with some wings absorbed by the interstellar clumps in the hot interior at velocities intermediate between the shell velocity and the ambient interstellar velocity. Only the model with a clumpy medium and interior SNRs may produce high-velocity, red-shifted components in the C IV and N V absorption lines. For example, the model with a clumpy medium without any SNRs would produce C IV and N V absorption at velocities similar to the approaching side shell velocity, with some wings absorbed by the interstellar clumps in the hot interior at velocities intermediate between the shell velocity and the ambient interstellar velocity. Only the model with a clumpy medium and interior SNRs can produce high-velocity, red-shifted components

in the C IV and N V absorption lines. The off-center SNR model would produce high-velocity, blue-shifted components in the C IV and N V absorption lines, if the SNR shocks the approaching side of the superbubble shell.

The *IUE* high-dispersion archival data have been used to study the behavior of interstellar C IV absorption lines (Chu et al. 1994). Very few observations exist for stars in X-ray-bright superbubbles. At least in N51D, the interstellar N V absorption shows extended blue wings indicating high-velocity, shocked material, which supports the existence of a SNR (de Boer & Nash 1982). More high-quality, high-dispersion UV spectroscopic observations are needed to determine the real dominant mechanism to produce bright X-ray emission in superbubbles.

One interesting phenomenon that can be diagnosed by the  $10^6$  K gas revealed in X-ray images is the interstellar blowout. The X-ray image of the superbubble N44 shows bright, diffuse emission in the shell center, with excellent correspondence between the optical shell morphology and the distribution of X-ray emission, but it also shows an X-ray extension toward the southeast (Chu et al. 1993). At the position where the X-ray extension starts, the  $H\alpha$  image shows an opening in the shell and long filaments perpendicular to the shell periphery and extending beyond the shell boundary (Figure 3). This  $H\alpha$  morphology apparently supports the blowout nature.

### 3.3. Giant H II Region 30 Doradus

The giant H II region 30 Doradus is the most conspicuous diffuse X-ray source in the LMC (see Figure 2). The physical structure of 30 Dor is nevertheless quite easy to understand when both kinematic data (Chu & Kennicutt 1994) and X-ray images (Wang 1995) are available. There is an excellent correlation between shell structures and the diffuse X-ray emission. At the core region, the diffuse X-ray emission correlates with the fast expanding shells, while in the outer regions the diffuse X-ray emission correlates with large shell structures (see Figure 4). These large shell structures are essentially X-ray-bright superbubbles, although the 30 Dor shells are the only X-ray-bright superbubbles in which high-velocity shocked material has been detected in the  $H\alpha$  emission line (Chu & Kennicutt 1994). It is likely that the diffuse X-ray emission from 30 Dor is dominated by SNR activities; therefore, the filling factor must be considered carefully when deriving the amount of hot gas or thermal energy in 30 Dor.

### 3.4. Supergiant Shells

Supergiant shells are the largest interstellar structures in a galaxy. Since their sizes ( $\sim 1000$  kpc) exceed the presumed scale height of the gaseous disk of a galaxy, they provide sites for mass and energy to be transported to large distances from the galactic plane. Supergiant shell blowouts are considered one of the most important mechanisms responsible for a hot gaseous halo around a galaxy.

Are supergiant shells really filled with hot, ionized gas? Two of the LMC supergiant shells, LMC2 (Wang & Helfand 1991b) and LMC4 (Bomans, Dennerl, & Kürster 1994), have been detected in X-rays. The *Einstein* data of LMC2 are too noisy for reliable plasma temperature analysis, and the *ROSAT* data have not been reported yet. The analysis of *ROSAT* PSPC observations of LMC4 yields a plasma temperature of  $2.4 \times 10^6$  K (Bomans et al. 1994). The total thermal energy in LMC4 calculated from their results is about  $10^{53}$  erg.

### 3.5. Large-Scale Structures

Comparison between the  $H\alpha$  image (Figure 1) and the X-ray image (Figure 2) of the LMC shows a great deal of large-scale diffuse X-ray emission that does not have any interstellar counterpart in the  $H\alpha$  image. Some of the emission appears to be associated with the LMC bar; some has no counterpart at all, such as the  $1^\circ$ -long arc of diffuse emission to the east of N44; while others seem to be associated with outflows from energetic regions, such the X-ray arc to the north of 30 Dor and the bright X-ray spur to the south of the supergiant shell LMC2. Not much is known about the nature or origin of the large-scale distribution of  $10^6$  K gas yet.

## 4. DIRECTIONS FOR FUTURE WORK

Now is an opportune time to study hot ionized gas in the LMC, as high-quality *ROSAT* X-ray data are available for the analysis of the  $10^6$  K gas, high-spectral-resolution *ASCA* observations allow us to refine the X-ray analysis (plasma temperature and absorption) of the  $10^6$  K gas, and the *HST* GHRS is available for high-dispersion, high-quality UV interstellar absorption observations of the  $10^5$  K gas. To understand fully



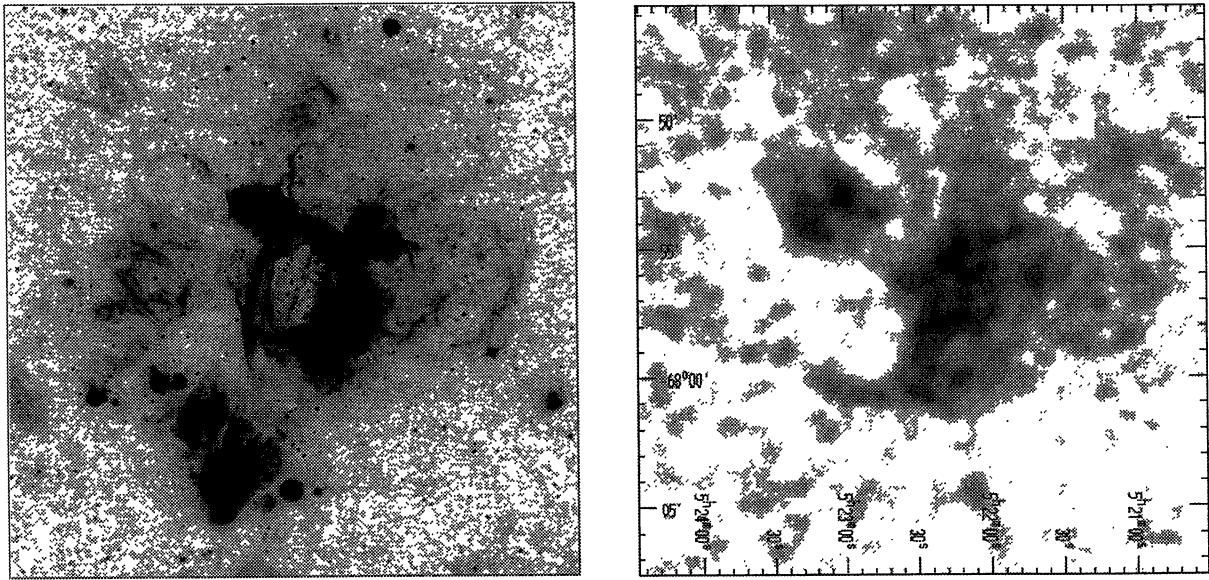


Fig. 3.  $H\alpha$  image (left) and a smoothed X-ray image (right) of N44. The  $H\alpha$  image is from the CCD survey by Smith et al. (1995). The X-ray image is produced from the *ROSAT* PSPC observation rp500093.

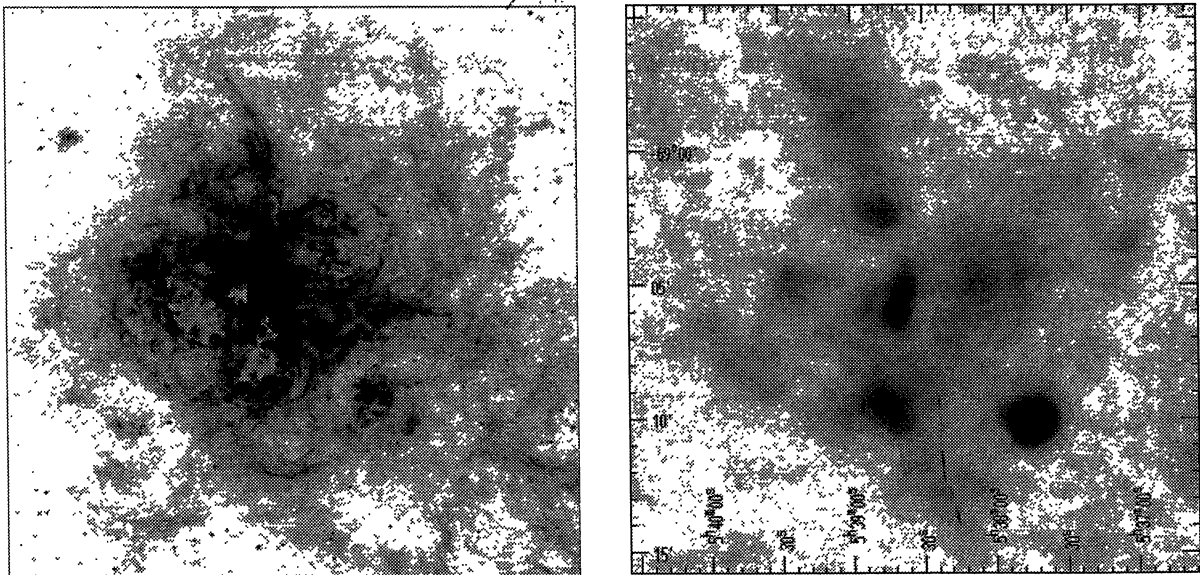


Fig. 4.  $H\alpha$  image (left) and a smoothed X-ray image (right) of 30 Dor. The  $H\alpha$  image is from the CCD survey by Smith et al. (1995). The X-ray image is produced from the *ROSAT* PSPC observation rp500131.

the physical conditions of an interstellar structure, we must study the different temperature components and determine their relationship. Since hot ionized gas is produced by massive stars, we must study massive stars alongside the ISM. While we *work* hard to analyze the abundant data available and extract physical parameters, we must remember to *think* harder about the physical significance of the results.

## REFERENCES

- Arthur, S. J., & Henney, W. J. 1995, MNRAS, submitted
- de Boer, K. S., & Nash, A. G. 1982, ApJ, 255, 447
- Bomans, D. J., Dennerl, K., & Kürster, M. 1994, A&A, L21
- Caplan, J., & Deharveng, L. 1985, A&AS, 62, 63
- Chu, Y.-H., Chang, H.-W., Su, Y.-L., & Mac Low, M.-M. 1995b, ApJ, in press
- Chu, Y.-H., Dickel, J. R., Staveley-Smith, L., Osterberg, J., & Smith, R. C. 1995a, AJ, 109, 1729
- Chu, Y.-H., & Kennicutt, R. C., Jr. 1994, ApJ, 425, 720
- Chu, Y.-H., & Mac Low, M.-M. 1990, ApJ, 365, 510
- Chu, Y.-H., Mac Low, M.-M., García-Segura, G., Wakker, B., & Kennicutt, R. C., Jr. 1993, ApJ, 414, 213
- Chu, Y.-H., Magnier, E., Cowley, A., Ögelman, H., Petre, R., Smith, R. C., Snowden, S., & Sanders, W. 1995c, in preparation
- Chu, Y.-H., Wakker, B., Mac Low, M.-M., & García-Segura, G. 1994, AJ, 108, 1696
- Davies, R. D., Elliott, K. H., & Meaburn, J. 1976, MNRAS, 91, 89
- Henize, K. G. 1956, ApJS, 2, 315
- Kennicutt, R. C., Jr., Bresolin, F., Bomans, D., Bothun, G. D., & Thompson, I. B. 1995, AJ, 109, 594
- Kennicutt, R. C., Jr., & Hodge, P. W. 1986, ApJ, 306, 130
- Lasker, B. M. 1979, CTIO Contribution No. 127
- Laval, A., Le Coarer, E., et al. 1995, in IAU Colloquium No. 149, in press
- Mathewson, D. S., Ford, V. L., Dopita, M. A., Tuohy, I. R., Long, K. S., & Helfand, D. J. 1983, ApJS, 51, 345
- Mathewson, D. S., Ford, V. L., Dopita, M. A., Tuohy, I. R., Mills, B. Y., & Turtle, A. J. 1984, ApJS, 55, 189
- Mathewson, D. S., Ford, V. L., Tuohy, I. R., Mills, B. Y., Turtle, A. J., & Helfand, D. J. 1985, ApJS, 58, 197
- Smith, R. C., Chu, Y.-H., Mac Low, M.-M., Oey, M. S., & Klein, U. 1994, AJ, 108, 1266
- Smith, R. C., Winkler, F., Chu, Y.-H., & Kennicutt, R. C. 1995, in preparation
- Snowden, S. L., & Petre, R. 1994, ApJ, 436, L123
- Wang, Q. D. 1995, ApJ, in press
- Wang, Q. D., Hamilton, T., Helfand, D. J., & Wu, X. 1991, ApJ, 374, 475
- Wang, Q. D., & Helfand, D. J. 1991a, ApJ, 373, 497
- \_\_\_\_\_ 1991b, ApJ, 379, 327
- Weaver, R., McCray, R., Castor, J., Shapiro, P., & Moore, R. 1977, ApJ, 218, 377